OPEN ACCESS
JOURNAL OF ADVANCED DIELECTRICS
Vol. 13, No. 2 (2023) 2350005 (6 pages)

DOI: 10.1142/S2010135X23500054

# High quality crystal growth and characterization of ferroelectric $Ba_{0.77}Ca_{0.23}TiO_3$ single crystal*

Lei Liu[†], Fangyi Yin[†], Guiyuan Zhao[†], Limei Zheng[†,‡,¶,**], Xiuwei Fu[†,‖,**], Zhitai Jia[†,§] and Xutang Tao[†]

[†]*State Key Laboratory of Crystal Materials, Shandong University Jinan, Shandong 250100, P. R. China*

[‡]*School of Physics, Shandong University, Jinan, Shandong 250100, P. R. China*

[§]*Shandong Research Institute of Industrial Technology Jinan, Shandong 250100, P. R. China*

[¶]zhenglm@sdu.edu.cn

[‖]fxw@sdu.edu.cn

Received 3 December 2022; Revised 14 January 2023; Accepted 5 February 2023; Published 8 March 2023

$Ba_{0.77}Ca_{0.23}TiO_3$ (BCT) single crystal has been widely studied as a promising lead-free ferroelectric material. In this work, high-quality BCT crystal was successfully grown by the Czochralski (CZ) method. The as-grown crystal is crack-free and shows black coloration. It possesses a high dielectric stability over a wide temperature range, while the dielectric loss is rather small below 90°C. Furthermore, it possesses excellent ferroelectric properties with residual polarization strength ($P_r$) and coercive field ($E_c$) of 17.93 $\mu$C/cm$^2$ and 8.47 kV/cm, respectively. Besides, BCT crystal shows large electromechanical coupling factors, with $k_t$, $k_{31}$, $k_{33}$ and $k_{15}$ of 0.535, 0.254, 0.714 and 0.721, respectively. The piezoelectric coefficients $d_{31}$, $d_{33}$ and $d_{15}$ are measured to be −36.5, 130 and 246 pC/N, respectively.

*Keywords*: Lead-free piezoelectric material; oxides; crystal growth; Czochralski method.

## 1. Introduction

Nowadays, piezoelectric materials play an irreplaceable role in the modern information society and are widely used in various fields such as ultrasound, underwater sound, electronics, automatic control and machinery.[1–5] It is well known that lead-containing piezoelectric materials have been dominating the market due to their excellent piezoelectric properties and temperature stability.[6–8] However, considering the harm of lead element to the human body and environment, it is essential to investigate lead-free piezoelectric materials with superior performance.[9–12]

$BaTiO_3$ (BT) is a well-known material in numerous lead-free systems. BT-based ceramics have been widely studied due to their high dielectric constant, large electromechanical coupling coefficient, excellent mechanical quality factor and good chemical stability.[13] In addition, compared to ceramic materials, single crystal materials generally offer significant improvements in material properties. However, the phase transition of BT crystal at room temperature leads to a reduction of the temperature stability and operating temperature region.[14,15] Numerous methods have been proposed to mitigate the effects of the phase transitions on the crystal properties,[15–17] where the most effective solution is by doping the element Ca.[18] This approach makes BT crystal become a stable tetragonal phase[19] and enhances the ferroelectric and piezoelectric properties.[20] Furthermore, the addition of calcium has a positive effect on the crystal growth. In the $Ba_{1-x}Ca_xTiO_3$ system, the component $x = 0.23$ exhibits congruent melting behavior and can be grown by the Czochralski (CZ) method.[21]

So far, $Ba_{0.77}Ca_{0.23}TiO_3$ (BCT) crystals were grown by several methods including the CZ method, the laser-heated pedestal growth method, the flux method and the floating zone method.[20–24] The phase structures and transition temperatures of BCT crystal have been widely investigated, and its stable tetragonal phase structure over a wide temperature range makes it a promising candidate for lead-free ferroelectrics.[25] However, as reported, it is difficult to grow high-quality BCT crystal.[26] The growth of high-quality single crystal is necessary in order to study its ferroelectric properties, piezoelectric properties and applications. In this work, large-size and high-quality BCT single crystal has been grown successfully by the CZ method. In addition, piezoelectric, ferroelectric and dielectric properties have been systematically investigated.

*This paper was originally submitted to the Special Issue on Piezoelectric Materials and Devices published in December 2022.

**Corresponding authors.

## 2. Experimental Method

The BCT polycrystalline materials were synthesized by solid-state reaction. The reaction equation is as follows:

$$0.77BaCO_3 + 0.23CaCO_3 + TiO_2 = Ba_{0.77}Ca_{0.23}TiO_3 + CO_2. \quad (1)$$

The raw material powders $BaCO_3$ (Aladdin 99.99%), $CaCO_3$ (Aladdin 99.99%) and $TiO_2$ (Macklin 99.99%) were weighed in the stoichiometric ratio and thoroughly mixed. The powders were compacted with a cold isostatic press at a force of 2500 kg-force/cm$^2$. Then, calcination and solid-state reaction of raw materials were carried out in the air atmosphere at 1350°C for 48 h.

The BCT single crystals were grown by the CZ method. The sintered ceramics were loaded into an Iridium (Ir) crucible and melted by induction under 99%Ar+1%$O_2$ atmosphere. After holding for about 1 h, the single crystal was pulled using a $[100]_C$-oriented BCT seed under the fixed pulling speed and rotation rate of 0.8 mm/h and 12 rpm, respectively. The crystals are slowly removed from the melt after passing through the seed, shoulder, cylinder and tail stages.

The chemical compositions were determined by an X-ray fluorescence (XRF) analysis (Rigaku, ZSX primus II). The sample from the bottom part of as-grown crystal was prepared for measurement. Powder X-ray diffraction (XRD) measurements were carried out using a BrukerAXS D8 ADVANCE X-ray diffractometer equipped with Cu K$\alpha$ radiation. Based on the XRD test results, the crystal structure was refined by the software Fullprof. Laue back-reflection measurements were carried out using a real-time back-reflection Laue camera system (Multiwire MWL 120 with Northstar software) to quickly evaluate the crystal quality. The energy dispersive spectrometer (EDS) mappings were achieved by a field-emission scanning electron microscope (HITACHI S-4800). The ferroelectric properties were measured by a ferroelectric analyzer (PK CPE1801). A $[100]_C$-oriented sample with an area of 8.4 mm$^2$ and a thickness of 1 mm was used for measurements. The ferroelectric test was performed under a maximum electric field of 21 kV/cm at 1 Hz using an amplified bipolar waveform in air atmosphere. To measure the piezoelectric properties, different piezoelectric resonators were treated, as shown in Fig. 1, and polarized according to the polarization conditions, as shown in Table 1. Impedance analyzer (Aglient E4990A) and quasi-static $d_{33}$ measuring instrument (YE2730A) were used to measure the dielectric and piezoelectric properties.

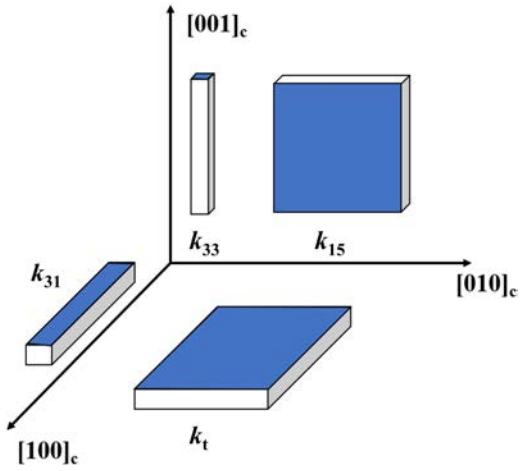


Fig. 1. Schematic diagram of standard cuts of different piezoelectric resonators (The blue area shows the gold electrode area).

Table 1. Polarization conditions for different piezoelectric resonators.

| Sample | $k_{33}$ | $k_{31}$ | $k_{15}$ | $k_t$ |
|---|---|---|---|---|
| Size (mm) | 1×1×5 | 5×1.5×0.5 | 1×5×5 | 2.5×2.5×0.5 |
| Intensity (kV/mm) | 1.5 | 2 | 1.5 | 2.5 |
| Temperature (°C) | Room temperature | | | |
| Time (min) | 15 | | | |
| Additional condition | Silicone oil | | | |

## 3. Results and Discussion

### 3.1. *Crystal growth*

High-quality BCT single crystal was successfully grown by the CZ method, as shown in Fig. 2. It can be seen that the as-grown crystal shows black coloration. Figure 3(a) shows the powder XRD patterns of BCT single crystal as well as BT for comparison. The obtained XRD pattern of BCT is essentially the same as that for the BT, but the peak positions are slightly shifted to the right, indicating that Ca ions with smaller radii replace Ba ions in the lattice. In addition, the Fullprof software was used to fit the XRD results of BCT single crystal. The calculated BCT crystal cell parameters are compared with the actual BT crystal parameters in Table 2, it was found that the *c/a* value of BCT is larger than that of BT, which confirmed that the Ca doping enhances the tetragonal nature of the BCT crystal. In order to further verify the successful doping of $Ca^{2+}$, the XRF test was carried out on the

Fig. 2. Photograph of as-grown BCT single crystal.

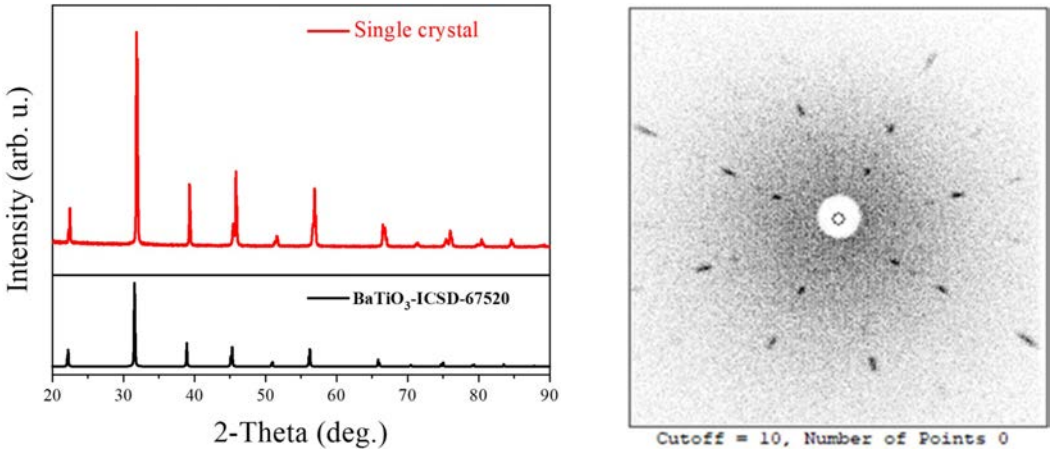


(a) (b)

Fig. 3. (a) Powder XRD patterns of BCT single crystal as well as BT for comparison and (b) Laue back-reflection of $(100)_C$ plane.

Table 2. Cell parameters and composition of BCT single crystal.

| Cell parameters | | | | |
|---|---|---|---|---|
| Crystal | $a = b$ | $c$ | $c/a$ | $\alpha = \beta = \gamma$ |
| BT[27] | 3.9998 | 4.018 | 1.0046 | 90° |
| BCT | 3.9695±0.002 | 4.0068±0.002 | 1.0094 | 90° |
| **Composition** | | | | |
| Element | | Ca | Ba | Ti |
| Mass fraction (%) | | 5.5807 | 65.1302 | 29.2891 |
| Mole ratios (%) | | 0.2270 | 0.7730 | 1 |

BCT plate, as shown in Table 2. The crystal composition can be calculated as $Ba_{0.77}Ca_{0.23}TiO_3$, which is consistent with the composition of polycrystalline materials.

The structural quality of the BCT crystal was characterized by a Laue back-reflection measurement. It is obviously seen from Fig. 3(b) that the Laue diffraction pattern is symmetric and clear, which shows high crystalline quality.

The single crystal XRD pattern of $[100]_C$-oriented plate was tested as shown in Fig. 4(a). The measured diffraction peaks are consistent with the standard $(100)_C$ ones. Additionally, the crystal uniformity was analyzed by field-emission scanning electron microscopy on $(100)_C$ crystal sample. Figure 4(b) illustrates the corresponding EDS mappings. It can be seen that the as-grown crystals exhibit excellent homogeneity.

### 3.2. *Dielectric and ferroelectric properties*

Figure 5(a) shows the variation of the dielectric constant and dielectric loss as a function of temperature under different frequencies (1 kHz, 10 kHz, 100 kHz and 1 MHz). As can be seen, there is a strong dielectric peak centered at 106°C for all frequencies, which is corresponding to the tetragonal-cubic

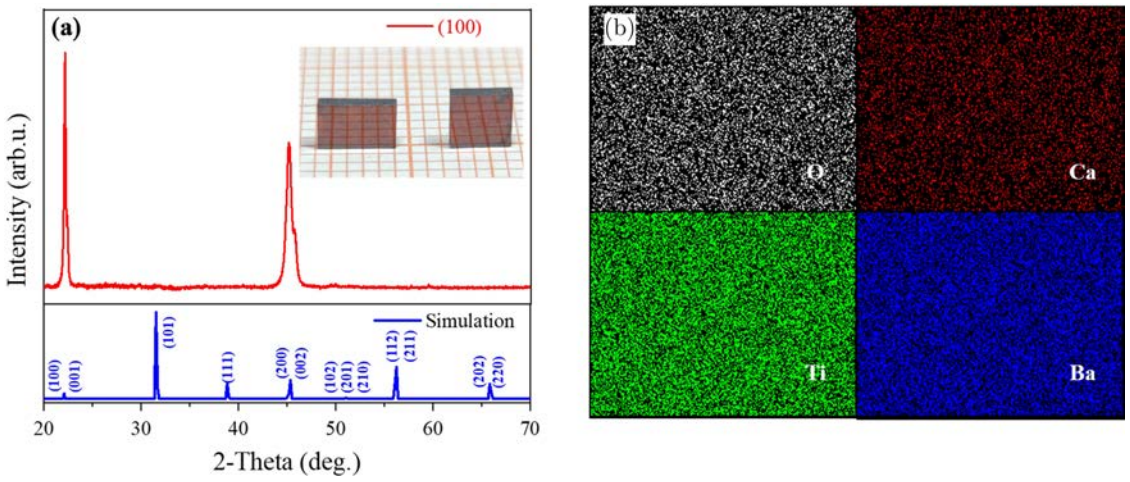


Fig. 4. (a) XRD patterns of $(100)_C$ plate and (b) Corresponding EDS mappings.

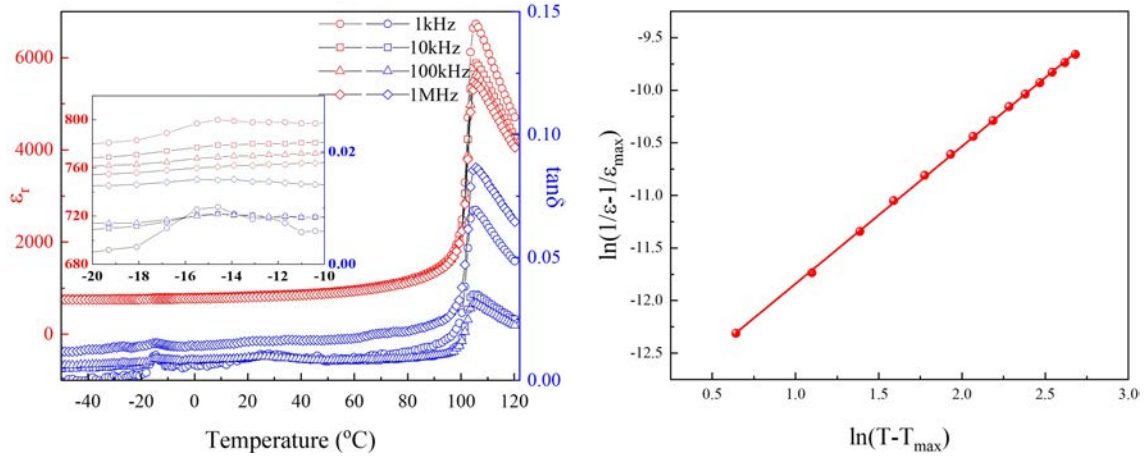


(a) (b)

Fig. 5. (a) The variation of dielectric constant and dielectric loss of BCT crystal with temperature and (b) Fitting diagram of the Curie–Weiss' law of BCT crystal.

phase transition (at $T_c$). Therefore, the Curie temperature of BCT is slightly lower than that of BT (120°C). On the other hand, the orthorhombic-tetragonal transition at around −15°C becomes negligible, indicating excellent dielectric stability for BCT crystal in the temperature range of −50–60°C. In addition, the dielectric constant gradually decreases with increasing test frequency, which on behalf of the different polarization mechanisms was stimulated at different frequencies. Meanwhile, there is no significant $T_c$ peak broadening, and the Curie points are consistent at all frequencies, indicating that the BCT crystal is not a typical relaxor ferroelectric. In order to figure out its ferroelectric nature, the fit analysis was performed using the modified Curie–Weiss law[28]:

$$\frac{1}{\varepsilon(T)} - \frac{1}{\varepsilon_{\max}} = \frac{(T - T_{\max})^{\gamma}}{C}, \tag{2}$$

where $\varepsilon(T)$ is the dielectric constant at temperature $T$, $\varepsilon_{\max}$ is the maximum value of dielectric constant as a function of temperature, $C$ is the Curie–Weiss coefficient, $T_m$ is the temperature corresponding to the maximum dielectric constant and $\gamma$ is coefficient of dispersion. The extreme values $\gamma = 1$ and $\gamma = 2$ correspond to the Curie–Weiss law (valid in the normal ferroelectric) and the quadratic law (valid in the ideal relaxation ferroelectric case), respectively.[29] The fitting diagram of the BCT single crystal is shown in Fig. 5(b). The value of $\gamma = 1.31$ was between 1 and 2, which proved that BCT is a conventional ferroelectric without obvious relaxation. Figure 5(a) also shows that the dielectric loss is less than 2.5% as the temperature rises from room temperature to 90°C, but increases rapidly near the $T_c$. The hysteresis loop of the BCT single crystal is shown in Fig. 6. The maximum polarization strength ($P_{\max}$) is 21.62 $\mu$C/cm$^2$, the residual polarization strength ($P_r$) is 17.93 $\mu$C/cm$^2$ and the coercive field ($E_c$) is 8.47 kV/cm. Its properties are similar to that of BT single crystal.[30]

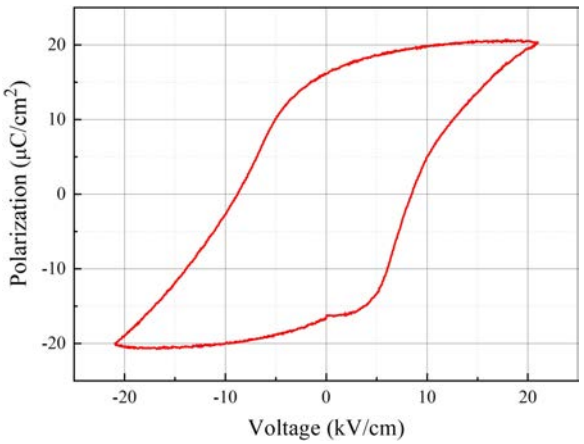


Fig. 6. Hysteresis loop of BCT sample in $[100]_C$ direction.

### 3.3. *Piezoelectric properties*

The electrical and elastic parameters are critical for piezoelectric materials. In order to study these parameters, four different piezoelectric resonators as described in the experiment section were prepared and polarized along $[001]_C$. After polarized, the tetragonal BCT crystal is in the 1T single domain state. Based on the matrix of symmetry, it can be seen that there are 11 independent dielectric, piezoelectric and elastic coefficients, including two independent dielectric coefficients, three independent piezoelectric coefficients and six independent elastic coefficients. In order to fully characterize the above parameters, the resonant and anti-resonant frequencies of the four polarized piezoelectric resonators were measured and calculated according to the following equations:

$$\varepsilon_{33}^{T} = \frac{Ct}{lw}, \quad \varepsilon_{11}^{T} = \frac{Ct}{lw}, \tag{3}$$

$$\frac{k_{31}^2}{1-k_{31}^2}=\frac{\pi f_a}{2f_r}tg\left(\frac{\pi\Delta f}{2f_r}\right),k_{33}^2=\frac{\pi f_r}{2f_a}tg\left(\frac{\pi\Delta f}{2f_a}\right),$$
$$k_{15}^2=\frac{\pi f_r}{2f_a}tg\left(\frac{\pi\Delta f}{2f_a}\right),k_t^2=\frac{\pi f_r}{2f_a}tg\left(\frac{\pi\Delta f}{2f_a}\right), \quad (4)$$

$$S_{11}^E=\frac{1}{4\rho\left(f_r l\right)^2},S_{11}^D=\frac{1}{4\rho\left(f_a l\right)^2},S_{33}^E=\frac{S_{33}^D}{1-k_{33}^2},$$
$$S_{33}^D=\frac{1}{4\rho(f_a l)^2},S_{55}^E=\frac{1}{C_{55}^E}, \quad (5)$$

$$d_{15}=k_{15}\sqrt{\varepsilon_{11}^T S_{55}^E},d_{33}=k_{33}\sqrt{\varepsilon_{33}^T S_{33}^E},d_{31}=k_{31}\sqrt{\varepsilon_{33}^T S_{11}^E}, \quad (6)$$

where $C$ is the capacitance at 1 kHz at room temperature, $l$, $w$ and $t$ correspond to the length and width of the piezoelectric resonator, respectively, $f_r$ and $f_a$ are the resonant and anti-resonant frequencies, respectively, and $\rho$ is crystal density (The density of 5.547 g/cm$^3$ was measured by drainage method at 26°C). The detailed test results are shown in Table 3.

The piezoelectric coefficient $d_{33}$ of BCT crystal measured by resonance method is 130 pC/N, almost the same as that value (123 pC/N) measured by the quasi-static $d_{33}$ measuring instrument. The dielectric constant $\varepsilon_{11}^T$ is 1234, about four times that of $\varepsilon_{33}^T$. The measured $d_{15}$ value is about 246 pC/N, significantly higher than that of $d_{31}$ and $d_{33}$. The BCT crystal possesses high electromechanical coupling coefficients, namely $k_{33}$ = 0.714 and $k_{15}$ = 0.721. In addition, the piezoelectric constant polarized along the $[011]_C$ direction was also measured by the quasi-static $d_{33}$ measuring instrument. It was found that the value along the $[011]_C$ direction is 150 pC/N, higher than the $[001]_C$ one.

Table 3. The piezoelectric, dielectric and elastic parameters of the BCT crystal measured at room temperature by the resonance method.

| Electromechanical coupling factors: $k_{ij}$ | | | | |
|---|---|---|---|---|
| | $k_t$ | $k_{31}$ | $k_{33}$ | $k_{15}$ |
| BCT | 0.535 | 0.254 | 0.714 | 0.721 |
| BT[31] | / | 0.315 | 0.560 | 0.570 |
| Dielectric constants: $\varepsilon_{ij}$ ($\varepsilon_0$) | | | | |
| | | $\varepsilon_{33}^T$ | | $\varepsilon_{11}^T$ |
| BCT | | 311.407 | | 1234.822 |
| BT | | 168 | | 2920 |
| Elastic compliance constants: $S_{ij}^E$ and $S_{ij}^D$ ($10^{-12}$ m$^2$/N) | | | | |
| | $S_{11}^E$ | $S_{11}^D$ | $S_{33}^D$ | $S_{55}^D$ | $S_{55}^E$ |
| BCT | 7.531 | 7.139 | 5.911 | 5.102 | 10.677 |
| BT | 8.05 | 7.25 | 10.8 | 12.4 | 18.4 |
| Piezoelectric coefficients: $d_{ij}$ ($10^{-12}$ C/N) | | | | |
| | | $d_{31}$ | $d_{33}$ | $d_{15}$ |
| BCT | | −36.5 | 130 | 246 |
| BT | | −34.5 | 85.6 | 392 |

## 4. Conclusion

In this work, high-quality and large-size BCT single crystal was successfully grown by the CZ method. The crystal is of good quality, free of macroscopic defects and cracking. XRD and XRF were used to analyze the structure and composition, which verified that $Ca^{2+}$ successfully replaced $Ba^{2+}$. Furthermore, the dielectric and piezoelectric properties were investigated. BCT is a conventional ferroelectric without obvious relaxation. It possesses high dielectric stability over a wide temperature range of −50–60°C. The dielectric loss is less than 2.5% from room temperature to 90°C. The maximum polarization strength, residual polarization strength and coercive field are 21.62 $\mu$C/cm$^2$, 17.93 $\mu$C/cm$^2$ and 8.47 kV/cm, respectively. The piezoelectric coefficients $d_{33}$ and $d_{15}$ are measured to be 130 and 246 pC/N, respectively, while the corresponding electromechanical coupling coefficients $k_{33}$ and $k_{15}$ are 0.714 and 0.721, respectively.

## Acknowledgments

We gratefully acknowledge financial support from the National Natural Science Foundation of China (Grant No. 52002218), the Natural Science Foundation of Shandong Province (Grant No. ZR2020QE031), the State Key Laboratory of Solidification Processing in NWPU (Grant No. SKLSP202209), the National Key Research and Development Program of China (Grant No. 2022YFB3605704) and the Qilu Young Scholars Program of Shandong University.

## References

[1]P. Ares, T. Cea, M. Holwill, Y. B. Wang, R. Roldán, F. Guinea, D. V. Andreeva, L. Fumagalli, K. S. Novoselov and C. R. Woods, Piezoelectric materials: Piezoelectricity in monolayer hexagonal boron nitride, *Adv. Mater.* **32**, 1905504 (2020).
[2]Y. Y. Lim, S. T. Smith and C. K. Soh, Wave propagation based monitoring of concrete curing using piezoelectric materials: Review and path forward, *NDT & E Int.* **99**, 50 (2018).
[3]M. Safaei, H. A. Sodano and S. R. Anton, A review of energy harvesting using piezoelectric materials: State-of-the-art a decade later (2008–2018), *Smart Mater. Struct.* **28**, 113001 (2019).
[4]K. Shibata, R. Wang, T. Tou and J. Koruza, Applications of lead-free piezoelectric materials, *MRS Bull.* **43**, 612 (2018).
[5]J. Wu, X. Gao, J. Chen, C. Wang, S. Zhang and S. Dong, Review of high temperature piezoelectric materials, devices, and applications, *Acta Phys. Sin.* **67**, 207701 (2018).
[6]M. Kang, W. Jung, C. Kang and S. Yoon, Recent progress on PZT based piezoelectric energy harvesting technologies, *Actuators* **5**, 5 (2016).
[7]T. R. Shrout and S. J. Zhang, Lead-free piezoelectric ceramics: Alternatives for PZT?, *J. Electroceram.* **19**, 113 (2007).
[8]L. Yang, H. Huang, Z. Xi, L. Zheng, S. Xu, G. Tian, Y. Zhai, F. Guo, L. Kong, Y. Wang, W. Lu, L. Yuan, M. Zhao, H. Zheng and

G. Liu, Simultaneously achieving giant piezoelectricity and record coercive field enhancement in relaxor-based ferroelectric crystals, *Nat. Commun.* **13**, 2444 (2022).
[9]M. Prakasam, P. Veber, O. Viraphong, L. Etienne, M. Lahaye, S. Pechev, E. Lebraud, K. Shimamura and M. Maglione, Growth and characterizations of lead-free ferroelectric KNN-based crystals, *Comptes Rendus Phys.* **14**, 133 (2013).
[10]D. S. Keeble, F. Benabdallah, P. A. Thomas, M. Maglione and J. Kreisel, Revised structural phase diagram of $(Ba_{0.7}Ca_{0.3}TiO_3)$-$(BaZr_{0.2}Ti_{0.8}O_3)$, *Appl. Phys. Lett.* **102**, 092903 (2013).
[11]M. Acosta, N. Novak, V. Rojas, S. Patel, R. Vaish, J. Koruza, G. A. Rossetti and J. Rödel, $BaTiO_3$-based piezoelectrics: Fundamentals, current status, and perspectives, *Appl. Phys. Rev.* **4**, 041305 (2017).
[12]J. Rödel, W. Jo, K. T. P. Seifert, E.-M. Anton, T. Granzow and D. Damjanovic, Perspective on the development of lead-free piezoceramics, *J. Am. Ceram. Soc.* **92**, 1153 (2009).
[13]A. H. Meitzler and H. L. Stadler, Piezoelectric and dielectric characteristics of single-crystal barium titanate plates, *Bell Syst. Tech. J.* **37**, 719 (1958).
[14]W. L. Bond, W. P. Mason and H. J. McSkimin, Elastic and electromechanical coupling coefficients of single-crystal barium titanate, *Phys. Rev.* **82**, 442 (1951).
[15]Z. Li, S. K. Chan, M. H. Grimsditch and E. S. Zouboulis, The elastic and electromechanical properties of tetragonal $BaTiO_3$ single crystals, *J. Appl. Phys.* **70**, 7327 (1991).
[16]K. Buse, F. Baller, R. Pankrath, H. Hesse and E. Krätzig, Photorefractive and related properties of $Ba_{0.984}Sr_{0.016}TiO_3$ crystals, *Solid State Commun.* **88**, 587 (1993).
[17]J. Zhuang, G. S. Li, X. C. Gao, X. B. Guo, Y. H. Huang, Z. Z. Shi, Y. Y. Weng and J. Lu, Preparation and photorefractive properties of barium strontium titanate $(Ba_{1-x}Sr_xTiO_3)$, *Opt. Commun.* **82**, 69 (1991).
[18]C. Kuper, R. Pankrath and H. Hesse, Growth and dielectric properties of congruently melting $Ba_{1-x}Ca_xTiO_3$ crystals, *Appl. Phys. A* **65**, 301 (1997).
[19]M. E. Savinov, V. A. Trepakov, S. Kamba, S. E. Kapphan, J. Petzelt, R. Pankrath, I. L. Kislova, A. B. Kutsenko and L. Jastrabik, Dielectric and infrared response of $Ba_{0.77}Ca_{0.23}TiO_3$, *Ferroelectrics* **295**, 31 (2003).
[20]D. Fu, M. Itoh and S. Koshihara, Crystal growth and piezoelectricity of $BaTiO_3$-$CaTiO_3$ solid solution, *Appl. Phys. Lett.* **93**, 012904 (2008).
[21]D. Fu, M. Itoh, S. Y. Koshihara, T. Kosugi and S. Tsuneyuki, Anomalous phase diagram of ferroelectric $(Ba,Ca)TiO_3$ single crystals with giant electromechanical response, *Phys. Rev. Lett.* **100**, 227601 (2008).
[22]S. Ralakumar, R. Ilangovan, C. Subramanian and P. Ramasamy, Growth of $Ba_{1-x}Ca_xTiO_3$ single crystals and their characterisations, *Ferroelectrics* **158**, 115 (2011).
[23]R. Varatharajan, R. Jayavel and C. Subramanian, Growth and characterization of ferroelectric $Ba_{1-x}Ca_xTiO_3$ single crystals, *Ferroelectrics* **215**, 169 (1998).
[24]L. B. Barbosa, D. R. Ardila and J. P. Andreeta, Crystal growth of congruent barium calcium titanate by LHPG, *J. Cryst. Growth* **231**, 488 (2001).
[25]Y. Wen, C. He, L. Ye, X. Zhu, C. Deng, R. Xu, Z. Chen, H. Yang, F. Wang, Y. Lu and Y. Liu, Growth and electrical properties of lead-free ferroelectric single crystal $Ba_{0.77}Ca_{0.23}TiO_3$, *Ceram. Int.* **48**, 25628 (2022).
[26]X. Xie, Z. Huang, Y. Kong, L. Zhang, S. Liu, S. Chen, X. Li, D. Zhao, L. Xiao and J. Xu, Study on the growth and optical properties of barium calcium titanate crystal, *J. Synth. Cryst. (China)* **34**, 242 (2005).
[27]R. H. Buttner and E. N. Maslen, Structural parameters and electron difference density in $BaTiO_3$, *Acta Crystallograph. B Struct. Sci.* **48**, 764 (1992).
[28]K. Uchino and S. Nomura, Critical exponents of the dielectric constants in diffused-phase-transition crystals, *Ferroelectrics* **44**, 55 (2011).
[29]G. A. E. Smolenskii, Physical phenomena in ferroelectrics with diffused phase transition, *J. Phys. Soc. Jpn.* **28**, 26 (1970).
[30]Z. Dan, D. Lin, T. H. He, Z. Y. Feng, H. Q. Xu and H. S. Luo, Investigation on electro-strain effect in Rh-doped $BaTiO_3$ single crystals, *Acta Phys. Sin.* **54**, 4053 (2005).
[31]D. Berlincourt and H. Jaffe, Elastic and piezoelectric coefficients of single-crystal barium titanate, *Phys. Rev.* **111**, 143 (1958).